### Communication

Lingyu Meng, Ming Hu\* and Keming Jia

# Fabrications and microstructure analysis of cobalt-based coatings by an easy-coating and sintering process

https://doi.org/10.1515/secm-2022-0178 received September 24, 2022; accepted December 18, 2022

Abstract: In order to enhance the service life of special complex shaped workpieces under severe working conditions, a new coating preparation process, namely, easycoating and sintering technology, has been proposed. In this study, the feasibility of preparing Co-based coatings on 38CrMoAl substrates using the easy-coating and sintering process was investigated, and the microstructure and properties of the Co-based coatings were studied. By optimizing the parameters of the sintering process, the prepared coating is dense, and the coating forms a good metallurgical bond with the substrate with few pores, but no other defects. As the process has good applicability to the surface of complex-shaped parts, the inner wall of small serpentine tubes and large thicknesses, and is low-cost and easy to operate, the easy-coating-sintering process has great application prospects.

**Keywords:** Co-based powder, coatings, easy-coating and sintering process, microstructure, property

# 1 Introduction

38CrMoAl alloy steel is a kind of high-grade nitriding steel, with high surface hardness and abrasion resistance. Due

\* Corresponding author: Ming Hu, School of Materials Science and Engineering, Jiamusi University, Jiamusi, 154007, P. R. China; Engineering Research Center of Metal Wear Resistance Materials and Surface of Technology of Ministry of Education, Jiamusi, 154007, P. R. China, e-mail: minghu02@jmsu.edu.cn, tel: + 86-13846158051

Lingyu Meng: School of Materials Science and Engineering, Jiamusi University, Jiamusi, 154007, P. R. China

Keming Jia: School of Materials Science and Engineering, Jiamusi University, Jiamusi, 154007, P. R. China; Engineering Research Center of Metal Wear Resistance Materials and Surface of Technology of Ministry of Education, Jiamusi, 154007, P. R. China

to its advantages of high strength, good resistance and corrosion resistance, and being relatively cheap, it is always preferred [1]. Due to its broad application prospects in pipeline, auto industry, chemical industry, and other fields, this steel has received a great deal of attention from materials scientists [2–7]. In order to achieve the performance requirements of technical pipes and tubes, 38CrMoAl alloy steel needs to have a high surface hardness and corrosion resistance, to extend its service life [8]. Therefore, improving the wear resistance and corrosion resistance of 38CrMoAl alloy steel has become one of the hot spots of research.

Most of the research has focused on improving the alluvial corrosion resistance of 38CrMoAl steels by controlling the temperature and adding rare earth elements to achieve extended applications [9,10].

All of the above methods can improve the wear and corrosion resistance of 38CrMoAl substrates, but by conventional surface modification methods, it is difficult to achieve the desired results under harsh operating conditions. Li et al. [11] used laser hybrid plasma spraying (LHPS) to deposit WC-10Co4Cr coatings on 38CrMoAl substrates and tested the wear and corrosion resistance of the coatings. It was found that the LHPS coating had fewer pores and cracks, which improved the wear resistance and corrosion resistance of the coating. One researcher also deposited a top diamondlike carbon (DLC) film on the surface of a 38CrMoAl steel substrate coated with Cr<sub>3</sub>C<sub>2</sub>-NiCr and showed that the wear resistance of the DLC/Cr<sub>3</sub>C<sub>2</sub>-NiCr double-layer coating was nearly ten times better than that of the single DLC film [12]. From this, it can be found that adding a coating to the 38CrMoAl substrate can effectively improve its performance, but for complex-shaped parts, there are greater difficulties in preparing the coating on its surface to achieve the expected results, so it is necessary to explore a new surface coating technology.

Among them, cobalt (Co)-based alloys are known for their high fatigue strength, corrosion resistance, and wear resistance at high temperatures [13–15], and the influence of the microstructure and processing methods of Co-based alloys on corrosion has been recognized [16,17]. This material is suitable for use on the surface of 38CrMoAl alloyed steel. Pascal et al. [18] combined a martensitic steel (X3CrNiMo13-4) and a Co-based alloy by sintering to form a corrosion and wear resistant bimaterial. By infiltrating the Co-based alloy super-solid into the steel, the two materials formed a mutual diffusion layer, and the mutual diffusion between the elements during sintering caused the two materials to form a diffusion layer to achieve a tight bond among the coating and substrate. The sintering method is also applicable on 38CrMoAl alloy steel; however, no reports have been found on the preparation of coatings on 38CrMoAl steels by the easy-coating and sintering method.

This study presents a new technique for preparing Cobased coatings by an easy-coating and sintering method. The process does not require complex equipment, only a special stirrer, syringe, and vacuum sintering furnace. This process is particularly suitable for a wide range of complex curved shapes. For fine size tubes, complex shaped parts, and especially the inner walls of small serpentine tubes, a thin and uniform coating can be obtained. So far, few reports have used similar coating preparation methods.

# 2 Experimental

The chemical composition (mass %) of the Co-based powder is as follows, Mo 22–20, Cr 19–21, Ni 14–16, Si 3.5–4.5, and the rest was cobalt. The substrate is 38CrMoAl steel with dimensions of 100 mm  $\times$  50 mm  $\times$  5 mm. The chemical composition (mass%) of 38CrMoAl steel is as follows, C 0.35–0.42, Cr 1.35–1.65, Mo 0.15–0.25, Al 0.70–1.10, Si 0.2–0.45, Mn 0.3–0.6, and S  $\leq$ 0.035, the rest was Fe. Due to the high density and weight of the powder, the ratio of Co-based powder to chemical reagents is 5.5–6.5 kg:1 L, in order to make the slurry (a kind of specially designed

chemical agents for coating metal powder) homogeneous and viscous when proportioning the slurry and using a special mixer for mixing. After mixing, the slurry was applied to the substrate using a common syringe with the right size. To prevent the coating from cracking or peeling off from the substrate, three heating stages were required during the sintering process. The temperatures were 600–650, 800–850, and 950–1,130°C in turn, each with a holding time of 20–30 min, the third holding stage was determined by the coating thickness, the cooling stages were 800–850 and 600–650°C, each stage was held for 20–30 min, then the furnace was cooled to 150°C, the door was opened, and the furnace was removed for natural cooling. The process for coating and sintering is illustrated in Figure 1.

The Co-based powder was heated to about 1,250°C at a rate of about 10°C/min under high-purity argon. The Co-based powder was heated at the same rate and subjected to differential scanning calorimetry (DSC).

### 3 Results and discussion

## 3.1 Thermodynamics and phase analysis

Figure 2(a) shows the DSC analysis curve of the Co-based powder. From the figure, it can be easily judged that the solid phase transition temperature of the cobalt alloy was determined to be 991°C, and the liquid phase transition temperature was 1,175°C, which are similar to that reported in ref. [19]. The weight loss rate of the Co-based powder initially increased gradually and then decreased with increasing temperature, which resulted from the melting for the Co-based powder.

Figure 2(b) shows the XRD patterns of the coating at different temperatures. Sintered at 1,085°C, the coating is

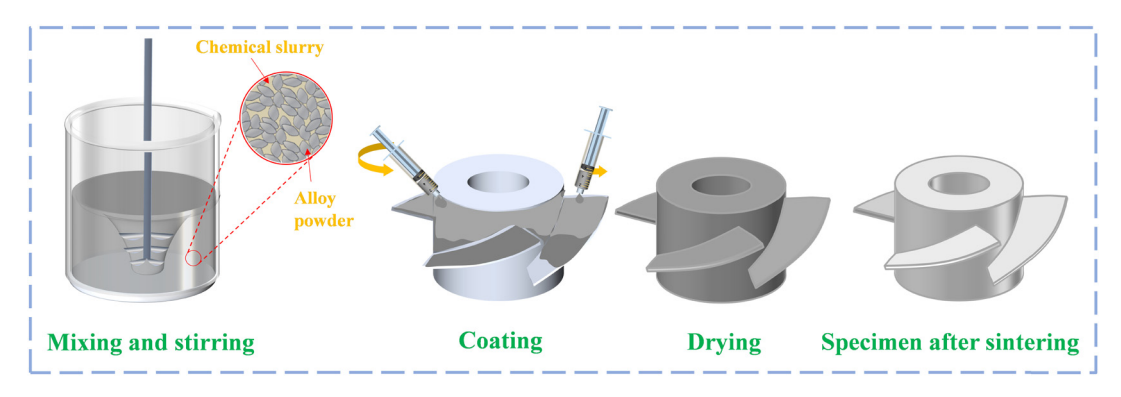


Figure 1: Schematic diagram of easy-coating and sintering process.

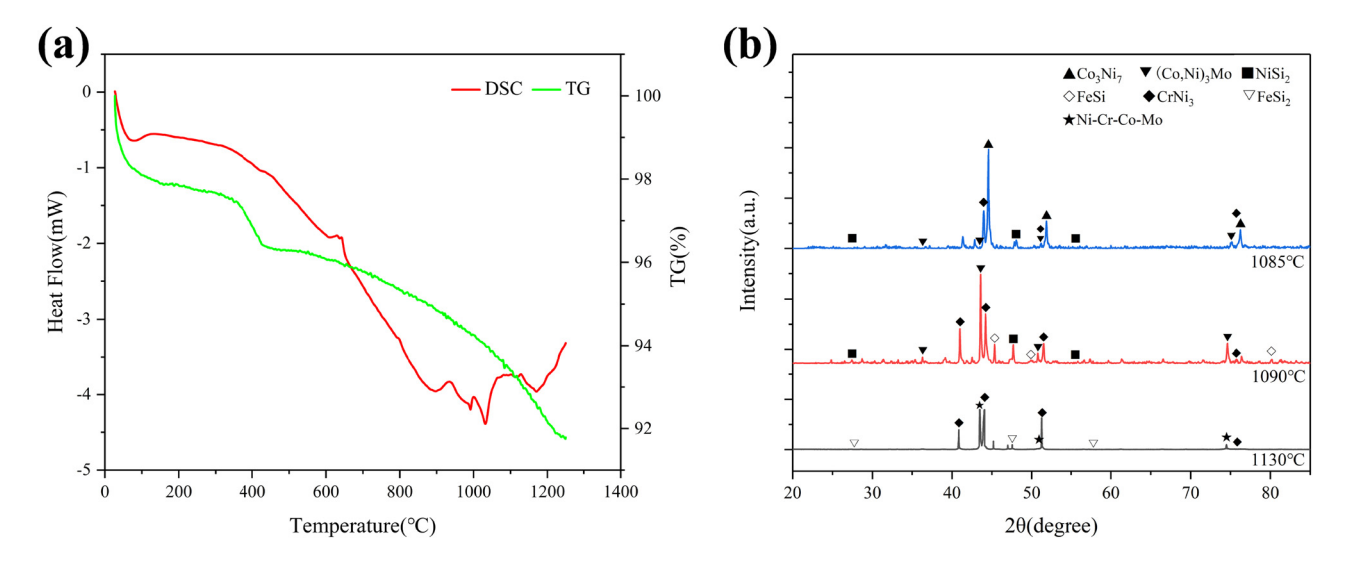


Figure 2: (a) The curves of the DSC analysis of the Co-based powder and (b) XRD patterns taken from the samples sintered at 1,085, 1,090, and 1,130°C.

mainly composed of Co<sub>3</sub>Ni<sub>7</sub> and CrNi<sub>3</sub> phases, with small amount of (Co,Ni)<sub>3</sub>Mo and tiny NiSi<sub>2</sub> phases, (Co,Ni)<sub>3</sub>Mo Lave phase is in cubic structure [20,21]. After being sintered at 1,090°C, the content of (Co,Ni)<sub>3</sub>Mo and CrNi<sub>3</sub> phases increased rapidly, small amount of NiSi<sub>2</sub> and FeSi phases were present in the coatings, while Co<sub>3</sub>Ni<sub>7</sub> phase almost disappeared. Subjected to sintering at 1,130°C, the coating consists mainly of CrNi<sub>3</sub>, FeSi<sub>2</sub>, and the Ni–Cr–Co–Mo phases formed by Cr, Ni, and Mo elements in a Co-based solid solution (PDF#00-035-1489), Co-based solid solution can be face-centered cubic [22]. It can be concluded that CrNi<sub>3</sub> phase is stable during the whole sintering process.

## 3.2 Microstructure analysis

The microstructures of the coating surfaces for specimens sintered at 1,085, 1,090, and 1,130°C are shown in Figure 3.

It can be seen that some powder melted and resolidified, individual particles were distributed in the coatings, and a few pores appeared during sintering at 1,085°C, the unmelted particles were bonded together by the molten liquid phase to form aggregates of particles, Figure 3(a). The XRD and EDS results confirmed that the gray part consisted of (Co,  $Ni)_3Mo$  and  $Cr_3Ni_7$  phases, shown in Figure 2(b) and Table 1, which is in accordance with the

**Table 1:** EDS analysis of different zones in the Co-based coating (wt%)

Region	Co	Cr	Мо	Ni	Si	Potential phases
1	27.05	30.51	21.54	14.72	0.00	(Co,Ni) <sub>3</sub> Mo and Cr <sub>3</sub> Ni <sub>7</sub>
2	63.19	8.83	1.31	22.42	4.25	(Co,Ni) <sub>3</sub> Mo and CrNi <sub>3</sub> and NiSi
3	26.22	35.61	34.62	3.54	0.00	Ni-Cr-Co-Mo
4	28.23	33.75	34.51	3.52	0.00	Ni-Cr-Co-Mo

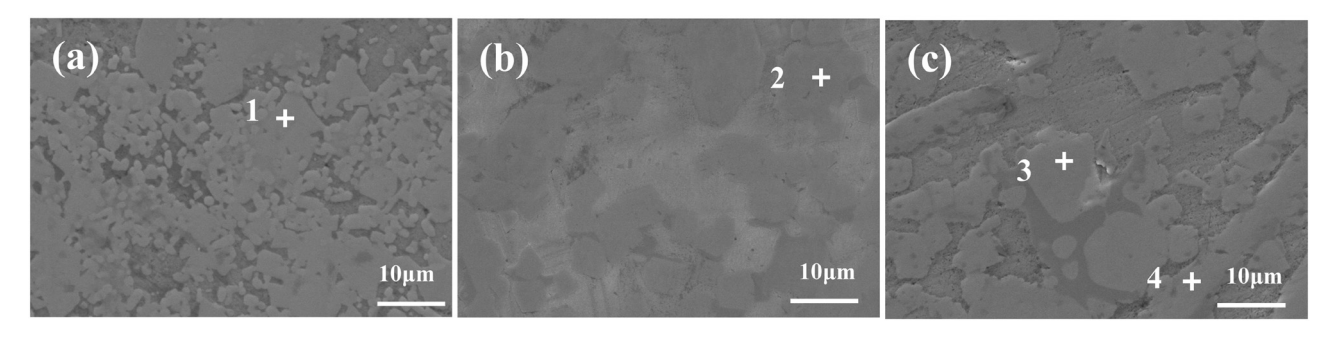


Figure 3: SEM images of Co-based coating surfaces at different sintering temperatures: (a) 1,085°C; (b) 1,090°C; and (c) 1,130°C.

reference [20]. This indicated that the diffusion ability of the atoms was poor, and sinter-ability of the powder was not strong at low temperature and short holding time. Most of the powder melted during sintering at 1,090°C. A continuous and dense coating was formed, and the discretely distributed particles and pores disappeared, the coating was characteristic of dendritic grains with more Co, Cr, and Fe elements, as shown in Figure 3(b). Combining XRD with EDS analysis results, it can be judged that the dark gray region consisted of (Co, Ni)3Mo and CrNi3 are main phases with small amount of NiSi<sub>2</sub> phase as shown in Figure 2(b) and Table 1. This indicated that the diffusion coefficients of Co and Mo elements increased with the rising the temperature. After the specimen was sintered at 1,130°C, the appearance of bulges and dendritic crystals formed from solidification of liquid metal could be seen in the coating [23], the dendritic grains grew and more Co, Cr, and Ni elements were present in the grains, as shown in Figure 3(c),

suggesting that sintering temperature was a little bit higher and more liquid phase appeared at 1,130°C. XRD and EDS results showed that the dendritic crystals were Ni–Cr–Co–Mo solid solution, Figure 2(b) and Table 1. As the sintering temperature increased, some grains of the Co-based coating changed from spherical-like to dendritic and the grain size increased [24].

The EDS line scans of the cross sections of the specimens at different sintering temperatures are shown in Figure 4. From Figure 4(a), it can be seen that some Co and Mo atoms immigrated from the coatings to the interface, and Fe atom diffused from the substrate to the interface [25]. A few carbon appeared in the interface between the coatings and substrate, which may suggest that tiny graphite was involved in the coatings during powder preparation.

The Co elements in the coating were much higher than in the matrix, small amounts of Co and Mo elements

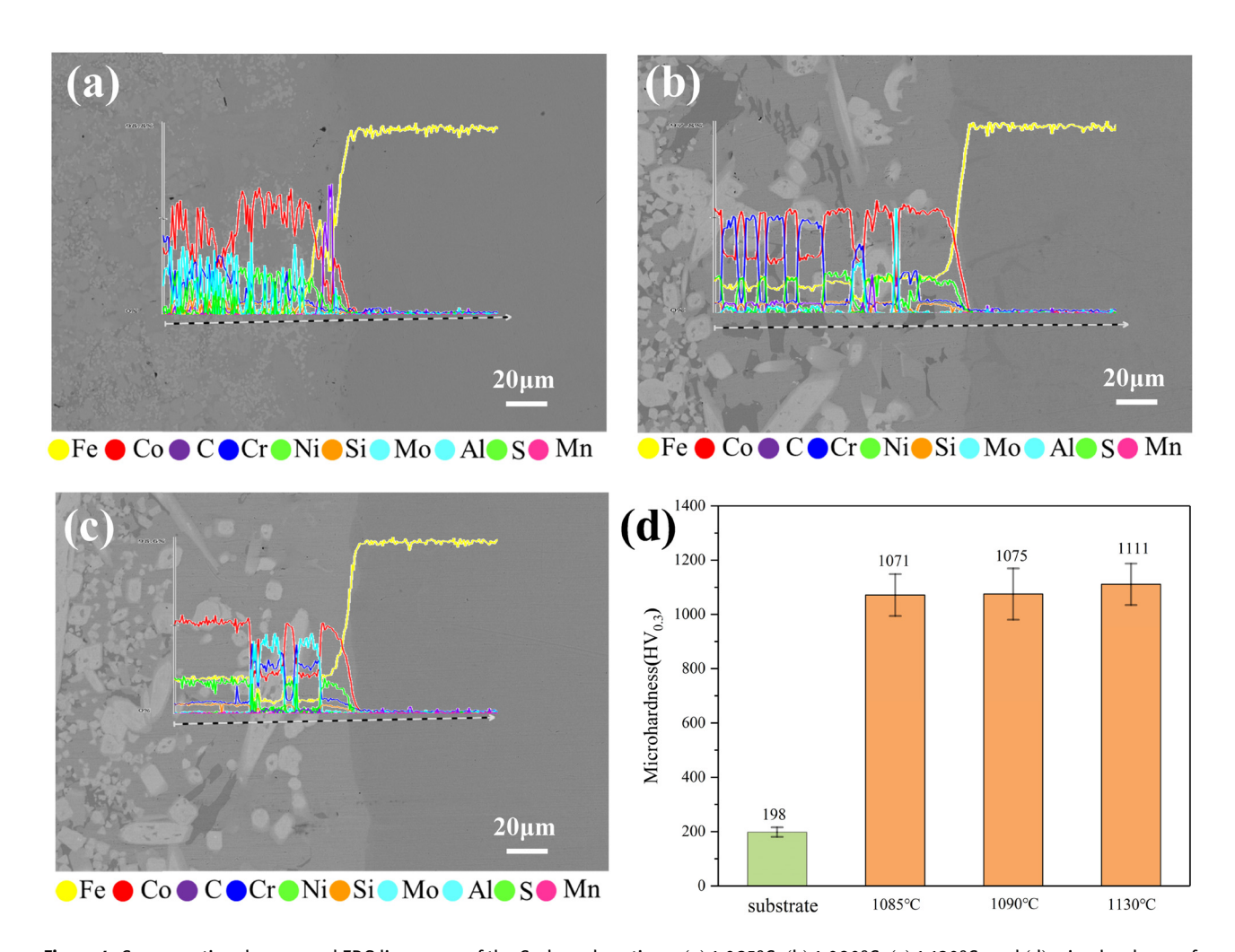


Figure 4: Cross-sectional scans and EDS line scans of the Co-based coatings: (a) 1,085°C, (b) 1,090°C, (c) 1,130°C; and (d) microhardness of coating.

diffuse into the interface, and Fe, the main element in the matrix, diffuses into the coating across the interface and reacts with Si elements to form the FeSi<sub>2</sub> phase, Figure 4(b). At 1,085°C, the interface between the coating and the substrate presents low levels of Co, Cr, Mo, Ni, and Si elements, while at 1,130°C, the content of elements around the interface increases, as shown in Figure 4(a) and (c).

As the sintering temperature increases, the higher the Cr, Mo, and Si atomic activity in the coating and Fe atoms in the substrate, and greater the inter-diffusion ability, which leads to the formation of some intermetallic compound and solid solution, such as (Co, Ni)<sub>3</sub>Mo, Cr<sub>3</sub>Ni<sub>7</sub>, CrNi<sub>3</sub>, and Ni–Cr–Co–Mo. And moreover, more Fe atoms diffuse from the 38CrMoAl matrix into the coating and react with Si to form FeSi<sub>2</sub>. This indicates a metallurgical bond between the coating and the 38CrMoAl matrix. The peak value of (Co, Ni)<sub>3</sub>Mo was higher at 1,090°C, indicating a higher content of dispersed hard phase at this temperature.

### 3.3 Microhardness analysis

Figure 4(d) shows the microhardness of the coatings at different sintering temperatures. It can easily be found that the hardness of the coatings is four or five times higher than the hardness of the substrate. With the increase in the sintering temperature, the hardness of the coatings increases. The microhardness of the coatings is 1,071 HV $_{0.3}$  and 1,075 HV $_{0.3}$  at 1,085 and 1,090°C, respectively. The highest hardness of the coating reaches around 1,111 HV $_{0.3}$  at 1,130°C. The high hardness is attributed to the increased solubility of Mo and the large number of CrNi $_3$  phases and Mo-rich intermetallic compounds in the coating, which also ensures that the material has good wear resistance even under severe working conditions [26]. This further demonstrates the effectiveness and reliability of the coating sintering process.

### 4 Conclusions

Co-based coatings were successfully prepared by easy-coating and sintering methods at three sintering temperatures.

(1) The microstructures of the Co-based coatings are related to the easy-coating and sintering process. Sintered at 1,085°C, the coating consists mainly of Co<sub>3</sub>Ni<sub>7</sub> and CrNi<sub>3</sub> phases; after sintering at 1,090°C, the content of (Co, Ni)<sub>3</sub>Mo and CrNi<sub>3</sub> phases in the

- coating increases rapidly; sintered at 1,130°C, the coating consists mainly of CrNi<sub>3</sub> and Ni–Cr–Co–Mo solid solution.
- (2) The surface of the coating is dense and smooth with a metallic lustrum. It is found that as the sintering temperature increased, it is beneficial to accelerate the diffusion of elements in the coating into the matrix, which help to improve the interfacial bonding.
- (3) The average hardness value of the coating is 1,111 HV<sub>0.3</sub> sintered at 1,130°C. The presence of Ni–Cr–Co–Mo solid solution and CrNi<sub>3</sub> phases in the coating are the result of the change in hardness.

On the whole, the easy-coating and sintering process is easy to operate. The Co-based coatings obtained by the process have no visible defects on the surface and are highly hard. Next we can explore the corrosion resistance of the cobalt-based coatings prepared by coating sintering to strong acids. Although coatings can also be prepared on the surface of parts by chemical plating and electroplating, the bond strength of the coatings is low, and they are not suitable for use in severe service conditions. The easy-coating and sintering method can be used successfully to prepare coatings on complex parts and on the inner walls of fine tubes with small internal diameters, so the preparation of Co-based coatings by coating sintering has good prospects in the transport industry, the pipeline industry, and the chemical industry.

**Acknowledgments:** This program is supported by the National Natural Science Foundation of China (Grant No. 51271088) and Scientific Research Project of Education Department of Heilongjiang Province (2018-KYYWF-0924). Thanks to Mr. Haicheng Yu, Senior Engineer of Zhejiang Wenzhou Xingji Electric Co., Ltd, and Mr. Daoyuan Zhu of Canada for their strong support for this project.

**Conflict of interest:** We declare that we have no conflict of interest with other people or organizations.

# References

- [1] Akhtar M, Khajuria A, Sahu JK, Swaminathan J, Kumar R, Bedi R, et al. Phase transformations and numerical modelling in simulated HAZ of nanostructured P91B steel for high temperature applications. Appl Nanosci. 2018;8(7):1669–85.
- [2] Chen Y, Song L, Zhang CK, Ye XM, Song RG, Wang ZX, et al. Plasma nitriding without formation of compound layer for 38CrMoAl hydraulic plunger. Vacuum. 2017;143:98-101.

- [3] Sun GF, Tong ZP, Fang XY, Liu XJ, Ni ZH, Zhang W. Effect of scanning speeds on microstructure and wear behavior of laser-processed NiCr-Cr<sub>3</sub>C<sub>2</sub>-MoS<sub>2</sub>-CeO<sub>2</sub> on 38CrMoAl steel. Opt Laser Technol. 2016;77:80–90.
- [4] Ren XL, Wang R, Wei DQ, Huang YY, Zhang HQ. Study on surface alloying of 38CrMoAl steel by electron beam. Nucl Instrum Methods Phys Res Sect B. 2021;505:44-9.
- [5] Wei DQ, Guo JY, Xia TH, Wu H. Effects of TiN/Ni ratio on the surface alloying of scanning electron beam. Nucl Instrum Methods Phys Res Sect B. 2020;476:73–8.
- [6] Deng YS, Zhang BY, Luo WL. The fretting behaviour of a nitrided steel 38CrMoAl. Wear. 1988;125(1-2):193-204.
- [7] Khajuria A, Akhtar M, Bedi R. Boron addition to AISI A213/P91 steel: Preliminary investigation on microstructural evolution and microhardness at simulated heat-affected zone. Materialwiss Werkstofftech. 2022;53(10):1167-83.
- [8] Akhtar M, Khajuria A. The synergistic effects among crystal orientations, creep parameters, local strain, macro-microdeformation, and polycrystals' hardness of boron alloyed P91 steels. Steel Res Int. 2022;93:2100819.
- [9] Yang L, He YY, Mao JY, Zhang L. Corrosion Behavior of Active Screen Plasma Nitrided 38CrMoAl Steel under Marine Environment. IOP Conf. Ser. Mater. Sci. Eng. Vol. 241. Issue 1. IOP Publishing; 2017. p. 012008.
- [10] Liu DJ, You Y, Yan MF, Chen HT, Li R, Hong L, et al. Acceleration of Plasma Nitriding at 550 °C with Rare Earth on the Surface of 38CrMoAl Steel. Coatings. 2021;11(9):1122.
- [11] Li SQ, Gong SL, Duan YP, Liu SH. Studies of laser hybrid plasma spraying WC-10Co4Cr coatings. Surf Eng. 2014;30(1):1-5.
- [12] Li WS, Zhao YT, He DQ, Song Q, Sun XW, Wang SC, et al. Optimizing mechanical and tribological properties of DLC/ Cr<sub>3</sub>C<sub>2</sub>-NiCr duplex coating via tailoring interlayer thickness. Surf Coat Technol. 2022;434:128198.
- [13] Silva HR, Ferraresi VA. Effect of cobalt alloy addition in erosive wear and cavitation of coatings welds. Wear. 2019:426:302-13.
- [14] Jiang D, Cui HZ, Song XJ, Zhao XF, Chen H, Ma GL, et al. Corrosion behavior of CoCrNiMoBC coatings obtained by laser cladding: Synergistic effects of composition and microstructure. J Alloy Compd. 2022;911:164984.

- [15] Uţu ID, Hulka I, Kazamer N, Constantin AT, Mărginean G. Hot-Corrosion and Particle Erosion Resistance of Co-Based Brazed Alloy Coatings. Crystals. 2022;12(6):762.
- [16] Karimi GN, Carrington MJ, Thomas J, Shipway PH, Stewart DA, Hussain T. The role of microstructural development in the hydrothermal corrosion of cast and HIPed Stellite 6 analogues in simulated PWR conditions. Corros Sci. 2019;159:108141.
- [17] Kamardan MG, Zaidi NHA, Dalimin MN, Zaidi AMA, Jamaludin SB, Jamil MMA. The sintering temperature effect on the shrinkage behavior of cobalt chromium alloy. Am J Appl Sci. 2010;7(11):1443.
- [18] Pascal C, Thomazic A, Antoni-Zdziobek A, Chaix J. Co-sintering and microstructural characterization of steel/cobalt base alloy bimaterials. J Mater Sci. 2012;47(4):1875–86.
- [19] Mane RB, Panigrahi BB. Comparative study on sintering kinetics of as-milled and annealed CoCrFeNi high entropy alloy powders. Mater Chem Phys. 2018;210:49-56.
- [20] Boulnat X, Lafont C, Coudert JB, Dayot C. Microstructure evolution of fine-grained cobalt T400 Tribaloy processed by Spark Plasma Sintering or Hot Isostatic pressing of gas-atomized powders. Metall Mater Trans A. 2020;51(10):5318-27.
- [21] Mason SE, Rawlings RD. Effect of iron additions on microstructure and mechanical properties of Ni-Cr-Mo-Si hardfacing alloy. Met Sci J. 1994;10(10):924-8.
- [22] Alidokht SA, Gao Y, De Castilho BCNM, Sharifi N, Harfouche M, Stoyanov P, et al. Microstructure and mechanical properties of Tribaloy coatings deposited by high-velocity oxygen fuel. J Mater Sci. 2022;57(42):20056-68.
- [23] Barekat M, Shoja Razavi R, Ghasemi A. Wear behavior of lasercladded Co-Cr-Mo coating on γ-TiAl substrate. J Mater Eng Perform. 2017;26(7):3226–38.
- [24] Veerappan G, Ravichandran M, Mohanavel V, Pritima D, Rajesh S. Effect of Copper on Mechanical Properties and Corrosion Behavior of Powder Metallurgy Processed Ni-Co-Cr-Fe-Mn-Cu<sub>x</sub> High Entropy Alloy. Arab J Sci Eng. 2022;47(7):1-11.
- [25] Kurt B, Somunkiran I. Interface microstructure of porous Ni-Ti and Co-Cr-Mo powder alloy couple fabricated by SHS process. Powder Metall. 2013;51(3):254-6.
- [26] Rogal Ł, Szklarz Z, Bobrowski P, Kalita D, Garzeł G, Tarasek A, et al. Microstructure and mechanical properties of Al-Co-Cr-Fe-Ni base high entropy alloys obtained using powder metallurgy. Met Mater Int. 2019,25(4):930-45.